

REORGANIZATION OF BRAIN ACTIVITY FOR MULTIPLE INTERNAL MODELS
AFTER SHORT BUT INTENSIVE TRAININGHiroshi Imamizu¹, Satomi Higuchi^{1,2}, Akihiro Toda³ and Mitsuo Kawato¹¹ATR Computational Neuroscience Laboratories, Kyoto, Japan; ²Nara Institute of Science and Technology, Nara, Japan; ³Nagaoka University of Technology, Niigata, Japan)

ABSTRACT

Internal models are neural mechanisms that can mimic the input-output properties of controlled objects. Our studies have shown that: 1) an internal model for a novel tool is acquired in the cerebellum (Imamizu et al., 2000); 2) internal models are modularly organized in the cerebellum (Imamizu et al., 2003); 3) their outputs are sent to the premotor regions after learning (Tamada et al., 1999); and 4) the prefrontal and parietal regions contribute to the blending of the outputs (Imamizu et al., 2004). Here, we investigated changes in global neural networks resulting from the acquisition of a new internal model. Human subjects manipulated three types of rotating joystick whose cursor appeared at a position rotated 60°, 110°, or 160° around the screen's center. In a pre-test after long-term training (5 days) for the 60° and 160° joysticks, brain activation was scanned during manipulation of the three joysticks. The subjects were then trained for the 110° for only 25 min. In a post-test, activation was scanned using the same method as the pre-test. Comparisons of the post-test to the pre-test revealed that the volume of activation decreased in most of the regions where activation for the three rotations was observed. However, there was an increase in volume at a marginally significant level ($p < .08$) only in the inferior-lateral cerebellum and only for the 110° joystick. In the cerebral cortex, activation related to 110° decreased in the prefrontal and parietal regions but increased in the premotor and supplementary motor area (SMA) regions. These results can be explained by a model in which outputs of the 60° and 160° internal models are blended by prefrontal and parietal regions to cope with the novel 110° joystick before the 25-minute training; after the acquisition within the cerebellum of an internal model for the 110°, output is directly sent to the premotor and SMA regions, and activation in these regions increases.

Key words:

INTRODUCTION

It is common knowledge that cortical representations in sensory-motor areas are not fixed but are continuously modified by experience (see Buonomano and Merzenich, 1998). When a lesion is made such that an adult animal loses sensation from a particular area, the region of the cortex innervated by the missing nerves loses inputs. However, after several weeks, this region becomes active again, being innervated by other axons adjacent to the lesion. Changes in cortical representation also occur as a result of training for tasks that produce specific, differential patterns of activity in cortical sectors. Skill learning or repetitive tactile stimulation expands digit representations in the somatosensory cortex of monkeys (Jenkins et al., 1990) and humans (Elbert et al., 1995), and in the human primary motor cortex (Karni et al., 1995, 1998). Reorganization is also known in the cerebellum regarding phylogenetically older sensory-motor parts. That is, a fractured tactile map reorganizes after deafferentation of a particular body part in adult rats (Shumway et al., 1999).

In the past decade, a number of studies have revealed that the cerebellum contributes to higher cognitive functions. Some of the first examples of a clearly cognitive task were reports of language

processing and activation in the right lateral cerebellum (Petersen et al., 1989; Raichle et al., 1994). Since then, other studies (see Thach, 1996; Desmond and Fiez, 1998) have also pointed to cerebellar involvement in such cognitive tasks as working memory (Desmond et al., 1997) and problem solving (Grafman et al., 1992; Kim et al., 1994). Many studies (Desmond et al., 1997; Sakai et al., 1998; van Mier et al., 1998) have demonstrated that cognitive processing exists in the lateral part of the cerebellum. However, little is known about whether the organization of the lateral cerebellum and cerebro-cerebellar communication loop changes due to experience.

A recent positron emission tomography (PET) study on monkeys revealed that tool use activates a cerebro-cerebellar communication loop including the intraparietal sulcus (IPS) regions, the supplementary motor area (SMA), the premotor cortex, and the lateral cerebellum (Obayashi et al., 2001). Our previous study (Imamizu et al., 2000) demonstrated that an internal model for a novel tool (a rotated mouse whose cursor appeared in a position 120° rotated around the center of a screen) is acquired in lateral parts of the human cerebellum. Tamada et al. (1999) have shown that functional connectivity between the lateral parts and the premotor regions increased after acquisition of the internal model, suggesting that the internal model

1 sends outputs to the premotor regions. We
 2 investigated cerebellar activity after subjects
 3 learned how to use two novel tools (the rotated
 4 mouse and a velocity mouse whose cursor velocity
 5 was proportional to the mouse position) (Imamizu
 6 et al., 1998, 2003). The brain locations activated
 7 while using the two different tools were spatially
 8 segregated with a small overlap, suggesting that
 9 multiple internal models are acquired in a modular
 10 fashion. Our study (Imamizu et al., 2004) suggested
 11 that the dorsolateral prefrontal cortex, the insula
 12 and parietal regions contribute to the switching and
 13 selection of multiple internal models as “central
 14 executives” or “responsibility estimators” in a
 15 MODular Selection And Identification for Control
 16 (MOSAIC) model proposed for the learning and
 17 switching of internal models (Wolpert and Kawato,
 18 1998; Kawato and Wolpert, 1998a).

19 Here, using our experimental paradigm, we
 20 investigated the reorganization of internal models
 21 and changes in neural networks between the
 22 cerebellum and the frontal and parietal regions due
 23 to the acquisition of a new internal model. After
 24 long-term training with the two novel tools,
 25 subjects were briefly but intensively trained on the
 26 use of a third novel tool. Brain activities for the
 27 three types of tools were scanned before and after
 28 training for the third tool and compared.

29 A computer program mapping the joystick
 30 position to the cursor position makes the joysticks
 31 functionally different, and there is no difference in
 32 their form or fundamental manipulation. Although
 33 there might be some argument about whether we
 34 can consider them as entirely different “tools”, we
 35 can find common tools that have similar form but
 36 require a different skill. For example, scissors are
 37 similar to pliers in form and essential mechanism.
 38 However, pliers need a grip force in a direction
 39 parallel to the handle movements, while scissors
 40 need not only the grip force but also a force to
 41 antagonistically push the two edges. Each joystick
 42 in our experiment requires a different skill to
 43 control the cursor, depending on different mapping
 44 between the cursor movement and the joystick
 45 movement. Thus, our experimental paradigm can
 46 probe into how different skills for tool use are
 47 organized in the brain.

50 METHODS

52 *Subjects*

53
 54 Fourteen neurologically normal subjects (five
 55 females and nine males from 21 to 39 years of
 56 age) participated in the experiments. All were
 57 right-handed according to the Edinburgh
 58 handedness inventory (Oldfield, 1971). Informed
 59 written consent was obtained from each subject.
 60 The test protocols were approved by the ATR
 61 ethics committee.

Tasks

Basic task designs are the same as those used in our previous studies (Imamizu et al., 2000, 2003, 2004). The subjects moved a small crosshair cursor on the screen with a joystick and continuously tracked a moving target. They controlled the joystick with their right hand. The target was a small white square on a dark background and moved around within a square area subtending horizontal and vertical visual angles of 7.33° . The x - and y -components of the target trajectory were sums of sinusoids whose amplitude and frequency were pseudo-randomly determined. A portion of the target trajectory is shown by small rectangles in Figure 3.

The relationship between cursor position and the joystick angle was

$$\begin{pmatrix} x \\ y \end{pmatrix} = 0.12 \begin{pmatrix} \cos \theta & \sin \theta \\ -\sin \theta & \cos \theta \end{pmatrix} \begin{pmatrix} p \\ q \end{pmatrix}$$

where (x, y) denotes the cursor's screen coordinates (visual angle: $^\circ$) and (p, q) denotes the deviational angles of the joystick from the vertical axis in the left-right and the back-forth directions. θ was a rotational angle of 0° , 60° , 110° , or 160° . Figure 1 illustrates the correspondence between the direction of joystick movement and that of cursor movement under each rotation.

Procedures

All subjects underwent the following: 1) five days of long-term training for the 60° and the 160° joysticks; 2) a pre-test; 3) 25 min of short-term training for the 110° joystick; and 4) a post-test. Brain activity was scanned in the pre- and post-tests.

Five Days of Long-Term Training for the 60° and the 160° Joysticks

The subjects were trained for the tracking task under 60° and 160° conditions. During the five-day training sessions, brain activity was not scanned but the subjects performed the tasks lying on a bed just as they would later do in the magnetic resonance imaging (MRI) scanner. Within each session, a tracking task period (1.6 min) and a rest period (18 sec) were alternately repeated three times without changing the joystick type. As shown in Figure 2a, the subjects used the 0° joystick in the first session each morning and were then trained for either the 60° or 160° joystick in the subsequent eight sessions. Breaks between sessions lasted 5-10 min. After a 1-2 hour lunch break, the subjects used the 0° joystick in the first session of each afternoon, and were subsequently trained for the other 60° or 160° joystick in eight sessions. The accumulated tracking time over the five days was 192 min for the 60° and 160° joysticks.

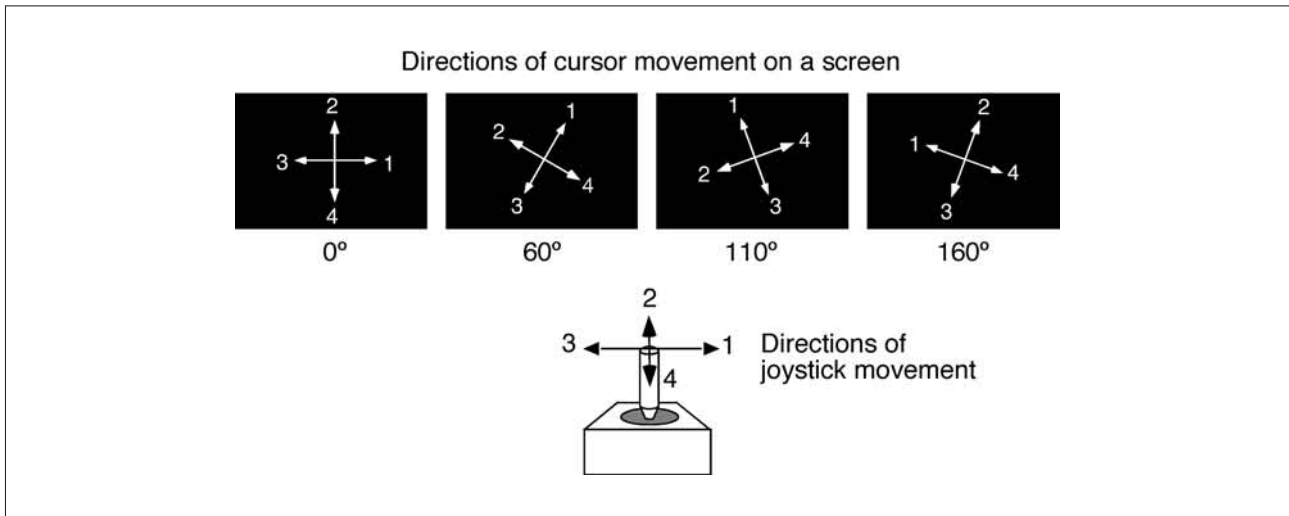


Fig. 1 – Relationship between the direction of joystick movements and that of cursor movements on the screen under each rotation. Black arrows indicate the direction in which subjects moved the joystick, while white arrows indicate the direction of the resulting cursor movement. Numbers indicate correspondence between the black and the white arrows.

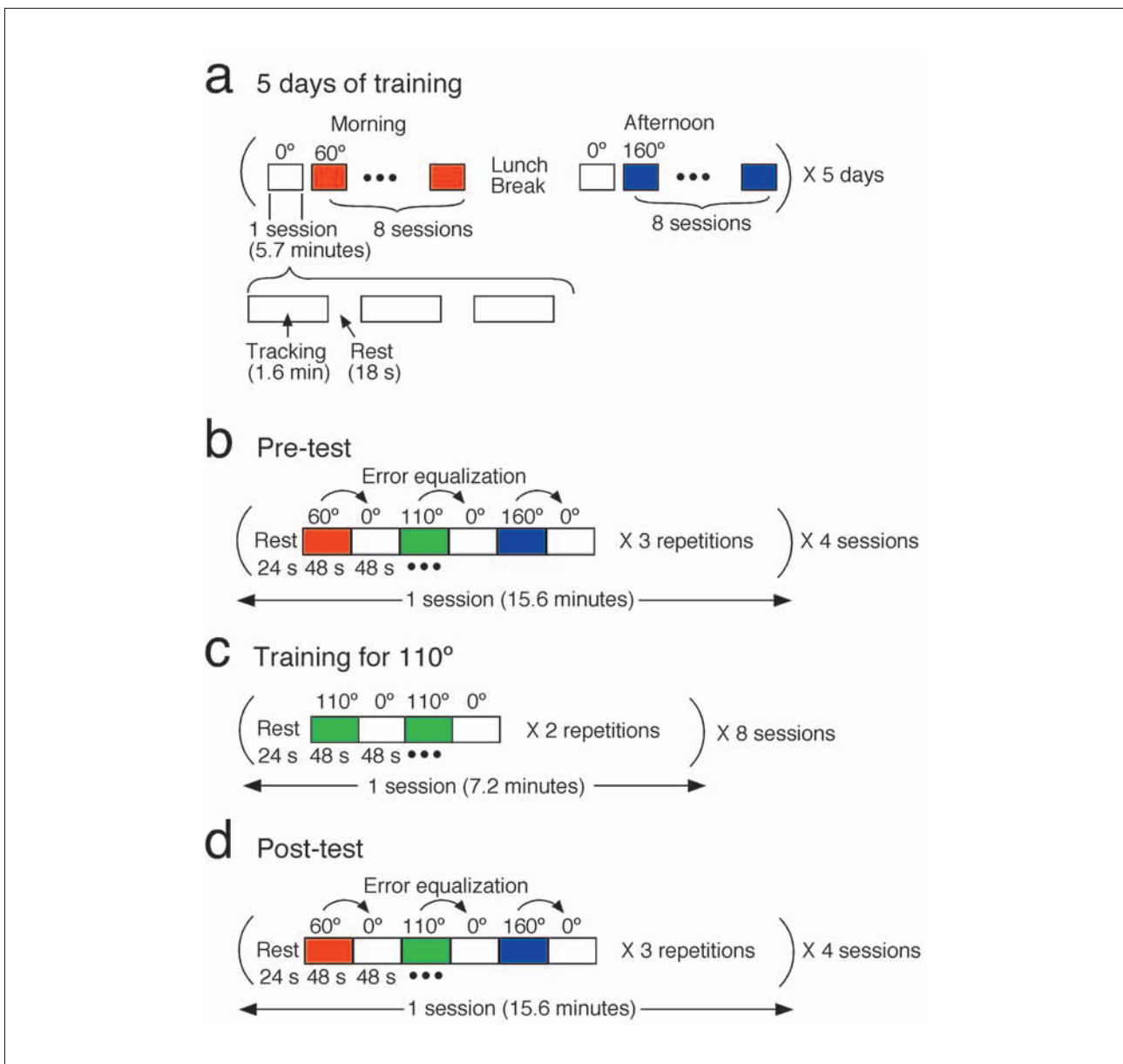


Fig. 2 – A graphic representation of the procedures in the present experiment.

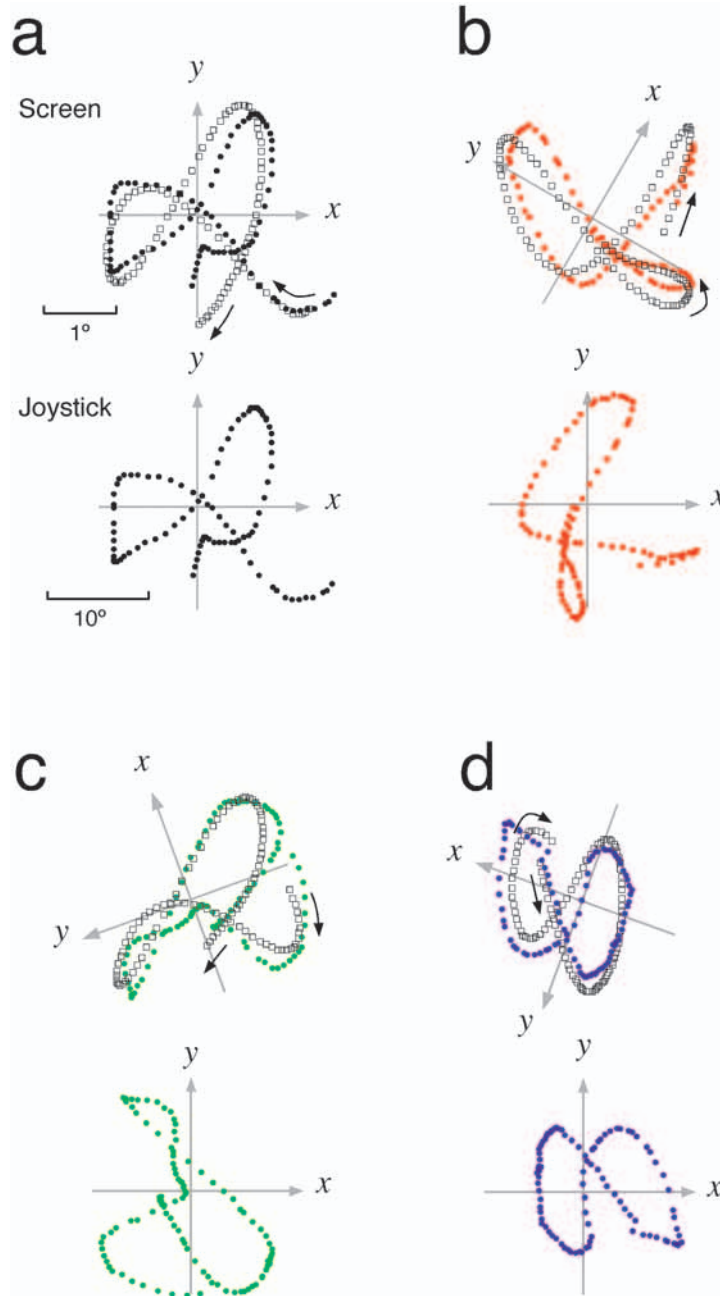


Fig. 3 – Examples of target trajectories (white rectangles) and joystick trajectories (filled circles) manipulated by a subject for 4 sec. a, b, c and d show trajectories when rotation angle was 0° , 60° , 110° , and 160° , respectively. Upper and lower panels show trajectories in the screen (visual angle: $^\circ$) and hand coordinates (deviational angle of the joystick from the vertical axis: $^\circ$). Marker positions are 40 msec apart.

Pre-Test

In a pre-test, the subjects used the 0° , 60° , 110° , and 160° joysticks in one session. The order of the tracking periods using these joysticks was counterbalanced between the sessions. An example of the session was three repetitions of [rest \rightarrow 60° \rightarrow 0° \rightarrow 110° \rightarrow 0° \rightarrow 160° \rightarrow 0°] as illustrated in Figure 2b. The rest period lasted 24 sec, while the other periods lasted 48 sec. When the subjects used the 0° joystick, the target velocity was adjusted so that the tracking error was equalized to the error for the joystick

used in the preceding period (see *Equalization of Tracking Error*). The subjects underwent four sessions.

25 Minutes of Short-Term Training for 110° Joystick

One session (7.2 min) was comprised of two repetitions of [rest \rightarrow 110° \rightarrow 0° \rightarrow 110° \rightarrow 0°] as shown in Figure 2c. The rest periods lasted 24 sec, while each tracking period lasted 48 sec. The subjects underwent eight sessions with 5-10-minute breaks between sessions. The accumulated tracking time for 110° joystick was short (25 min) in

comparison to that for 60° or 160° in the five days of long-term training (192 min).

Post-Test

The subjects underwent the same sessions as in the pre-test.

Analysis of Behavioral Data

The cursor, the target, and the joystick angles were sampled at 1 kHz. The distance between the cursor and the target at each sampling point ($\sqrt{(x_t - x_c)^2 + (y_t - y_c)^2}$) was accumulated over 5.3 sec (position tracking error). A velocity tracking error ($\sqrt{(x_t - x_c)^2 + (y_t - y_c)^2}$) was also accumulated over 5.3 sec. Because the results obtained from the velocity error were similar to those from position tracking error, we only present the position tracking error in this article.

Equalization of Tracking Error

In our previous study (Imamizu et al., 2000), two types of activities related to learning were observed in the cerebellum. One reflected error signals that guide the learning acquisition of internal models and the other reflected an acquired internal model. The former activity was so strongly distributed over the cerebellum that it also blurred the latter activity. Following the procedure used in the previous study, tracking error during manipulation of the normal (0°) joystick was equalized to that during the rotated joystick using a linear relationship between tracking error and target velocity. This procedure allowed us to distinguish internal model activity for the novel tools from activity reflecting the error signal.

Before functional imaging, the subjects performed the tracking task using the 0° joystick at various target velocities (V_0) that ranged from .0427 to .0783°/second at .0021 intervals. A linear relationship between V_0 and the tracking error (E) was derived by a least squares method for each subject:

$$E = aV_0 + b.$$

In the pre- and post-tests, the target velocity was adjusted using the estimated values a and b in the 0° baseline condition, so that the error was equal to the mean error (\bar{E}) in the preceding 60°, 110°, or 160° test periods:

$$V_0 = \frac{\bar{E} - b}{a}$$

The averaged target velocity was .0652°/second in the pre-test and .0543°/second in the post-test.

MRI Acquisition

A 1.5 T MRI scanner (Shimadzu-Marconi) was used to obtain blood oxygen level dependent

(BOLD) contrast functional images. Images weighted with the apparent transverse relaxation time were obtained with an echo-planar imaging sequence (repetition time = 5.3 sec, echo time = 65 msec, flip angle = 90°). A total of 158 sequential whole brain volumes (64 × 64 × 44 voxels at 3.4-mm isotropic resolution) were acquired in each session. High resolution anatomical images of all subjects were also acquired with a T1 weighted sequence.

MRI Analysis

We used Statistical Parametric Mapping 99 (SPM 99) software (<http://www.fil.ion.ucl.ac.uk/spm/>) for image processing and analysis. The first two volumes of images were discarded to allow for T1 equilibration while the remaining 156 image volumes were realigned to a reference volume. The first volume was chosen as the reference to minimize the difference between the realigned functional images and the anatomical image that was acquired immediately after subjects entered the MRI scanner. The realigned images were normalized to the Montreal Neurological Institute (MNI) reference brain. The data were spatially smoothed with a Gaussian kernel with a 7 mm full-width half-maximum (FWHM). The voxel time series were temporally smoothed with a Gaussian filter (FWHM of 4 sec).

We conducted a multiple regression analysis to find regions related to the manipulation of the three types of joysticks.

$$v_i^k = \alpha_i w^k + \beta_i x^k + \gamma_i y^k + \delta_i z^k + e_i$$

Here, v_i^k denotes the functional magnetic resonance imaging (fMRI) signal at the i -th voxel in the k -th scan, and w , x , y and z are explanatory variables corresponding to the use of the 0° (error equalized), 60°, 110°, and 160° joysticks, respectively. They were assigned 1 if the scan corresponded to their joystick type and 0 otherwise.

We performed a random effect analysis comprising two stages. In the first stage analysis, parameters were estimated for the differences of interest ($\beta - \alpha$, $\gamma - \alpha$ and $\delta - \alpha$) for each subject. They were then entered into a second-level analysis to test whether parameters for the 60°, 110°, or 160° joysticks were significantly larger than parameters for the error-equalized 0° joystick ($\beta - \alpha > 0$, $\gamma - \alpha > 0$ and $\delta - \alpha > 0$), using a one-sample t -test across subjects [$t(13) > 3.85$, $p < .05$ uncorrected].

Quantitative Analysis of Activity Change from Pre- to Post-Test

We searched for voxels in which activation was significantly associated with all three types of joystick. Then we identified the anatomical volume of interest (VOI) including the voxel according to (Tzourio-Mazoyer et al., 2002) and investigated the change in activated volume separately for each

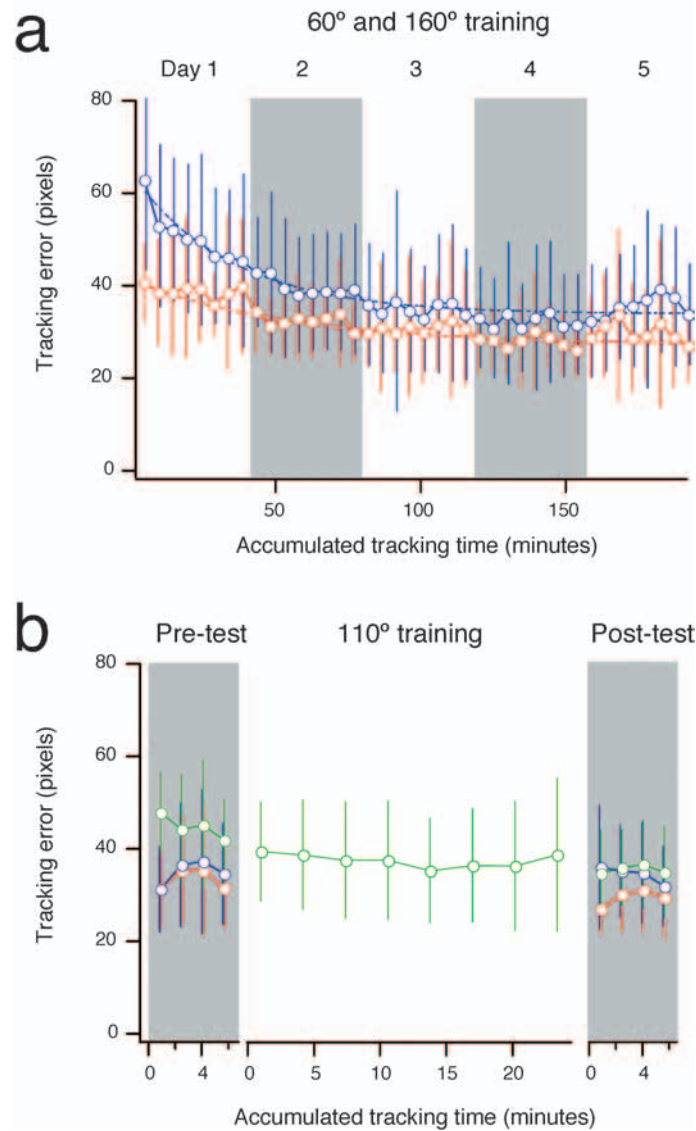


Fig. 4 – a. Change in tracking error (across-subjects mean \pm SD) during training sessions. Red and blue curves represent errors in 60° and 160° conditions, respectively. b. Pre-test, the 110° training, and post-test errors. The green curves represent errors in 110° condition.

VOI. The voxels were found in the premotor cortex and regions near the IPS. The premotor VOI was defined as Brodmann area 6, excluding the medial cortex but including both the ventral (PMv) and dorsal (PMd) parts. The parietal VOI comprised the superior parietal gyrus, the angular gyrus, the supramarginal gyrus, and the precuneus. The cerebellum was divided into upper and lower parts by a horizontal plane ($z = -40$) that roughly corresponded to the horizontal fissure.

RESULTS

Behavioral Data

Figure 3 shows a representative target and cursor trajectory from a subject's data while using each of the rotated angles. Although the target

trajectories were randomly determined and thus different for the four angles, the relationship between the target motion and the corresponding cursor motion was qualitatively the same.

Figure 4a shows how the tracking errors changed during long-term training for the 60° (red) and 160° (blue) joysticks before scanning. The errors for both joysticks decreased as the accumulated tracking time increased. A repeated measures analysis of variance (ANOVA) for errors indicated a significant time effect for the 60° joystick [$F(1, 39) = 1.76, p < .005$] and for the 160° joystick [$F(1, 39) = 3.25, p < .0001$], suggesting that learning had occurred.

Figure 4b shows errors during the pre-test, the short-term training for the 110° joystick, and the post-test. Using a paired t -test, we examined whether there was a significant difference between the errors in the pre- and post-tests. No significant

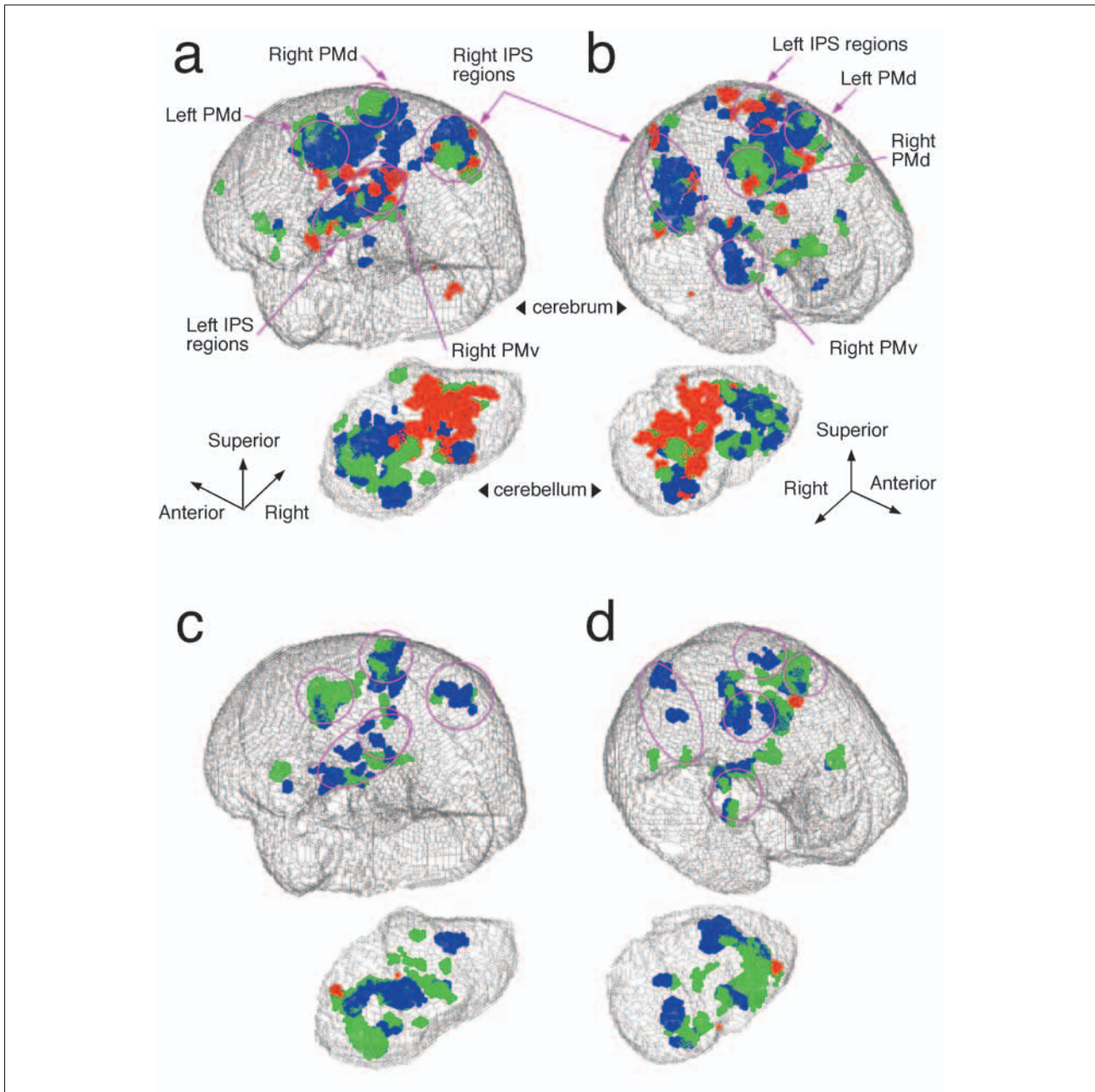


Fig. 5 – Brain activity related to 60° (red), 110° (green) and 160° (blue) conditions in pre-test (a and b) and post-test (c and d). Activity in error-equalized 0° condition was subtracted [random effect model, $t(13) > 3.85$, $p < .05$ uncorrected, cluster size > 10 voxels]. Activities are shown in left-superior-posterior view (a and c) and in right-superior-anterior view (b and d). The cerebrum and the cerebellum are separated into the upper and lower parts of each panel.

difference was observed for the 60° or 160° joystick [60°: $t(13) = .17$, 160°: $t(13) = 1.57$] but a significant decrease was observed for the 110° joystick [$t(13) = 3.83$, $p < .001$]. Thus, a significant effect of short-term training for the 110° training could be identified.

In the pre- and post-tests, target velocity was adjusted during the use of the 0° joystick to equalize tracking error to the error during use of the 60°, 110° and 160° joysticks (see *Equalization of Tracking Error* in Methods). There was no significant difference between these two equalized errors during both the pre-test and post-test for each type of joystick [60°: $t(13) = .64$, 110°: $t(13) = 1.19$, 160°: $t(13) = .97$ in the pre-test; 60°: $t(13)$

$= .24$, 110°: $t(13) = 1.55$, 160°: $t(13) = .57$ in the post-test], suggesting that error-equalization succeeded. The activations shown below were obtained by subtracting the corresponding 0° activation from the 60°, 110°, or 160° activation as explained in the MRI analysis section.

fMRI Data

Change of Three Types of Activation from Pre- to Post-Test

Figures 5a and 5b show the 60° (red), 110° (green), and 160° (blue) activations in the pre-test [$t(13) > 3.85$, $p < .05$ uncorrected, cluster size > 10

1
2
3
4
5
6
7
8
9
10
11
12
13
14
15
16
17
18
19
20
21
22
23
24
25
26
27
28
29
30
31
32
33
34
35
36
37
38
39
40
41
42
43
44
45
46
47
48
49
50
51
52
53
54
55
56
57
58
59
60
61

TABLE I
Regions activated in 110° condition and compared to error-equalized 0° condition

Anatomical description (Brodmann area)	R/L	Pre-test			Post-test			
		Coordinates	T-value	Voxels	R/L	Coordinates	T-value	Voxels
Frontal lobe (Lateral Surface)								
Superior frontal gyrus	(6) R	(22, 0, 52)	7.26	403	R	(20, -12, 58)	5.51	149
	(6) R				R	(24, -14, 74)	4.48	25
Middle frontal gyrus	(8) L	(-22, 8, 56)	5.14	42				
	(45) R	(48, 42, 22)	6.28	121				
	(46) L	(-38, 52, 24)	4.61	10				
Inferior frontal gyrus, Opercular Part	(44)				R	(62, 12, 26)	4.97	14
Frontal lobe (Medial Surface)								
Supplementary motor area	(6)				L	(-2, -14, 66)	4.46	12
Central region								
Precentral gyrus	(6) L	(-60, 10, 26)	5.91	37				
	(6) L	(-24, 14, 50)	5.79	229	L	(-28, -8, 58)	7.59	346
Rolandic operculum	(48)				R	(54, 10, 4)	4.97	54
Parietal lobe								
Supramarginal gyrus	(40) R	(40, -36, 42)	6.38	214	R	(64, -36, 32)	5.24	27
	(48) R	(58, -22, 28)	5.83	33	R	(56, -22, 28)	5.82	31
	(48) R	(58, -34, 28)	5.31	72				
Supramarginal gyrus	(6) L	(-58, -30, 36)	5.44	51				
Inferior parietal gyrus	(2) L	(-44, -32, 38)	4.72	13				
	(40) L	(-40, -42, 50)	5.10	32	L	(-34, -36, 42)	4.91	11
	(40) L	(-48, -48, 56)	4.88	12				
	(40) L	(-42, -40, 36)	4.18	12				
Precuneus	(7) R	(16, -74, 50)	5.86	50				
	(7) R	(16, -66, 58)	4.52	29				
Limbic lobe								
Median cingulate and paracingulate gyri	(6) R	(8, -6, 48)	6.39	214	R	(8, 10, 44)	5.85	169
Insula lobe								
Insula	(48) L	(-34, 16, 6)	4.68	14	L	(-28, 18, 10)	9.44	70
	(48) L	(-40, 14, -4)	4.93	11				
	(48) R	(42, 14, 0)	4.17	15				
Subcortical gray nuclei								
Thalamus		R (18, -6, 10)	4.49	12	R	(16, -12, 0)	7.62	291
		R (20, -18, 2)	5.97	217				
		L (-14, -8, 10)	5.44	33	L	(-14, -14, 8)	7.76	140
Lenticular nucleus pallidum		L (-8, 0, 2)	5.52	20				
Cerebellum								
Crus 1		L (-36, -46, -36)	8.62	369	L	(-48, -56, -40)	4.42	10
		L (-30, -70, -30)	5.91	85				
		R (24, -70, -30)	5.05	20				
		R (44, -50, -36)	4.73	19				
Lobule 3		L (-6, -26, -18)	6.54	138				
Lobule 4-5		L (-2, -44, -8)	5.42	26				
		L (-20, -26, -28)	4.55	13				
Lobule 6		R (28, -44, -32)	6.82	125	R	(34, -34, -34)	5.21	17
Lobule 7b		L (-16, -74, -46)	4.78	15	L	(-14, -74, -46)	4.96	11
					L	(-32, -46, -40)	8.82	686
Lobule 8		L (-24, -56, -54)	6.67	181	L	(-14, -58, -54)	4.63	34
					R	(16, -64, -32)	5.4	15
					R	(28, -46, -56)	6.13	118
Lobule 9		R (12, -62, -54)	6.17	29	R	(10, -34, -38)	5.53	28
Vermis 9					R	(10, -54, -32)	5.11	25

voxels]. Figures 5c and 5d show the activations in the post-test. The red (60°) regions decreased in the post-test in various regions, especially in the left and right intraparietal regions and the cerebellum. The green (110°) regions decreased in the cerebral cortex but increased in the inferior parts of the cerebellum. In the right ventral premotor cortex, in the pre-test the dominant color was blue (160°) but it was green (110°) in the post-test.

We searched for regions where the three types of activation (for 60°, 110° and 160°) overlapped in the pre-test and found them in the left premotor region, the left and right intraparietal regions, and the superior left and inferior right cerebellum. The

t -value weighted centers of gravity of those overlapping regions were (-27, -5, 51), (-37, -42, 45), (38, -35, 41), (-23, -66, -25) and (14, -61, -51), respectively. The number of voxels included in the regions were 6, 4, 19, 12 and 3. These regions are assumed to be closely related to the manipulation of the rotated joysticks.

Change of 110° Activity from Pre- to Post-Test

Table I lists the 110° activation peaks and peak t -values. A number of cerebral regions were activated in the pre-test but not all were significantly activated in the post-test. A decrease

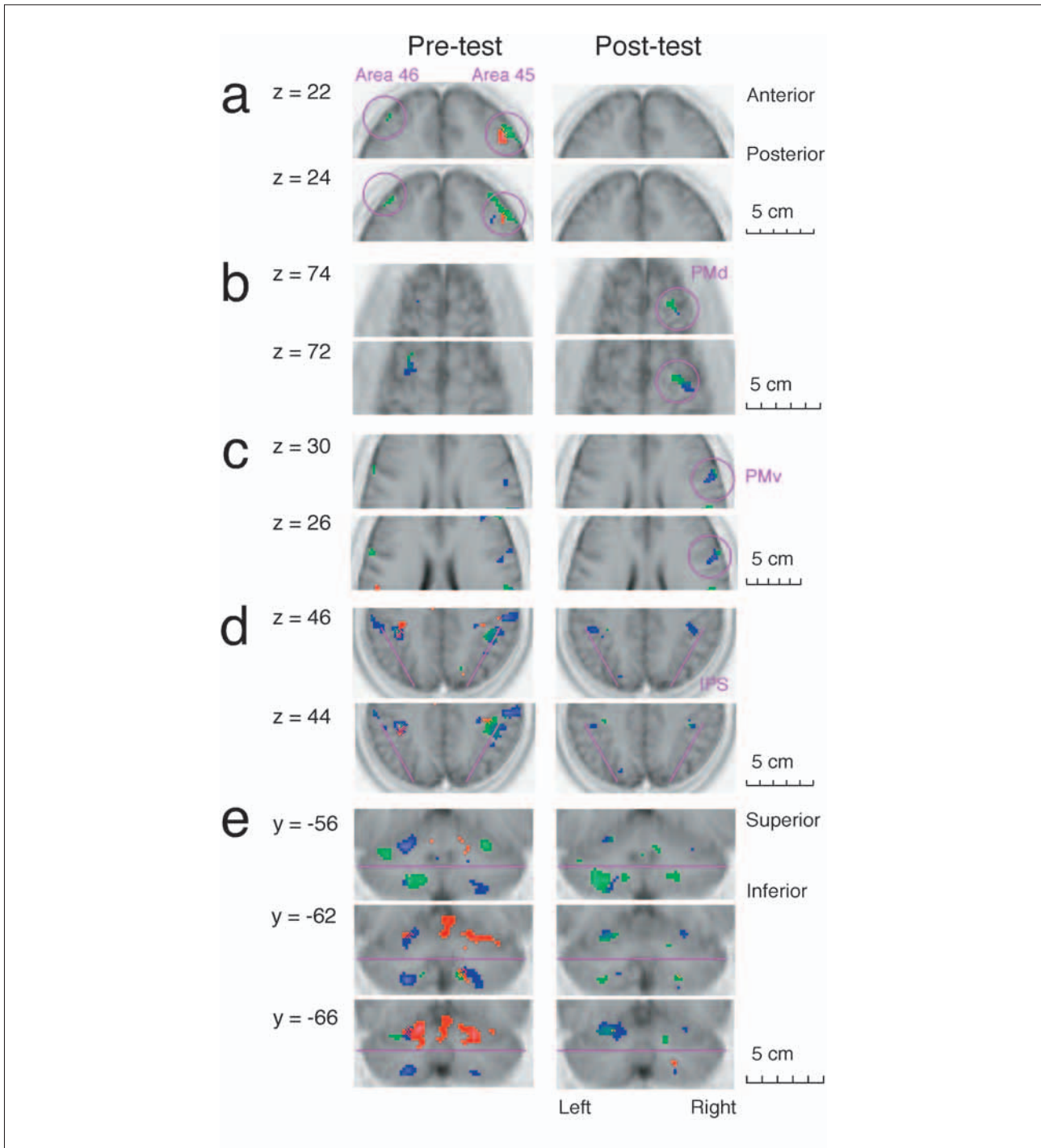


Fig. 6 – The same activities as in Figure 5 are shown in the transverse (a-d) or coronal sections (e). Sections include the prefrontal regions (areas 45 and 46) (a), the dorsal premotor cortex (b), the ventral premotor cortex (c), the intraparietal regions (d), and the cerebellum (e). Lines in e indicate the horizontal level at $z = -40$.

of activation was prominent in the prefrontal regions (area 6 in the superior frontal gyrus; areas 8, 45, and 46 in the middle frontal gyrus) and in the parietal regions. In contrast, an increase of activity was observed in the premotor (area 44 in the opercular part of the inferior frontal gyrus and area 6 in the superior frontal gyrus at $z = 74$ level) and in the SMA. The total number of voxels did not change drastically in the cerebellum. However, activation shifted from the superior parts (crus 1 and lobules 3-6) to the inferior parts (lobules 7b-9).

Figures 6a-6e show representative slices from the above regions. The panels in Figure 6a show areas 45 and 46 in the prefrontal regions where significant activation was observed in the pre-test but not in the post-test. Figures 6b and 6c include the dorsal and ventral premotor regions, respectively. Activation in the dorsal and ventral premotor regions increased in the post-test. Figure 6d shows the intraparietal regions where the 60° (red) and 110° (green) activations decreased in the post-test. Figure 6e shows the cerebellar activity in

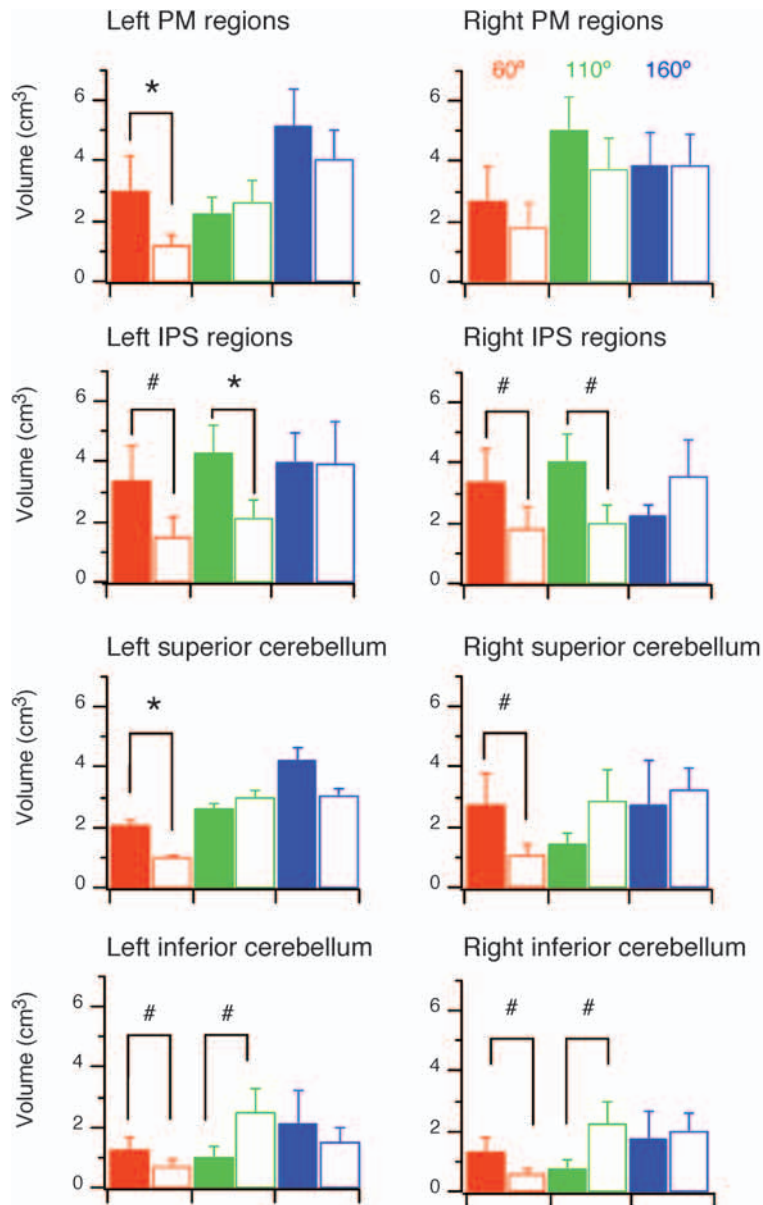


Fig. 7 – Activated volumes (across-subjects mean + SE) in anatomical regions where overlap among the 60°, 110°, and 160° activations was found in the pre-test. Threshold for activation was $t > 3.08$, $p < .05$ uncorrected (fixed effect model). Filled bars and open bars correspond to pre- and post-tests. * indicates $p < .05$, and # $p < .10$ according to a paired t-test.

the coronal sections. The 60° activation decreased in the superior parts, and the 110° activation increased in the inferior parts.

Quantitative Analysis of Change in Activity

We compared activated volume in the pre-test to that of the post-test for each subject for anatomical regions including the overlap among the three types of activation (Figure 7). The activated volume was measured in activation map of each subject ($p < .001$ uncorrected). This analysis was conducted not only in the regions where the overlap was found but also in the homologous region on the other side of the hemisphere. Below, we will describe increases or decreases thresholded at $p < .10$.

Although marginally significant (not significant in the strict sense) results pass this threshold, we will report them to indicate trends in change of activity.

Regarding the premotor regions, a significant volume decrease was found in the left premotor [$t(13) = 1.89$, $p < .04$, paired t -test] for the 60° activation. In the left and right intraparietal regions, a significant or marginally significant decrease was identified for the 60° activation [left: $t(13) = 1.45$, $p < .09$; right: $t(13) = 1.71$, $p < .06$] and the 110° activation [left: $t(13) = 1.85$, $p < .05$; right: $t(13) = 1.63$, $p < .06$]. The decrease in the 110° activation in the parietal regions was consistent with Table I. In the superior part of the cerebellum, the volume for the 60° activation decreased in the post-test [left: $t(13) = 1.92$, $p < .04$; right: $t(13) = 1.54$, $p < .10$].

.08] but the volume for the 110° activation increased [left: $t(13) = 1.65$, $p < .06$, right: $t(13) = 1.69$, $p < .06$]. Thus, an increase of activity at $p < .10$ level was only identified in the cerebellum.

We confirmed the above increase or decrease of volume for 110° activity in the post-test separately for each subject. When the activated volume was measured in the activation map of each subject ($p < .01$ uncorrected), the volume for 110° activity increased in the left or the right inferior cerebellum in 11 of the 14 subjects. Regarding those 11 subjects, we investigated change of the volume in the other regions of interest. The volume for the 110° activity increased in the left or right premotor region of six subjects and the SMA region of six subjects. The volume decreased in the left or right intraparietal region of eight subjects, the area-45 region of ten subjects, and the area-46 region in nine subjects.

DISCUSSION

In summary, the 110° activation in the frontal and parietal regions decreased in the post-test whereas it increased in the premotor (in the precentral gyrus and the opercular part of the inferior frontal gyrus) regions, in the SMA, and in the inferior part of the cerebellum. The 60° activation decreased in most of the brain regions. Regarding 160° activation, no significant change in activity was observed.

As mentioned in the Introduction, we previously investigated cerebellar activity on subjects who learned to use a 120° rotated mouse and identified activity reflecting an internal model separate from activity reflecting performance error. We used the same method to equalize tracking error as in the current experiment (Imamizu et al., 2000). We also previously investigated cerebellar activity after learning the use of two novel tools (a rotated mouse and a velocity mouse whose cursor velocity was proportional to the mouse's position). The activities of the two different tools were spatially segregated with slight overlap, suggesting that multiple internal models are acquired in a modular fashion (Imamizu et al., 2003).

The first advantage of possessing multiple internal models is the reduction of interference between different learning epochs, which enables the rapid switching of skilled behaviors. The second advantage is being able to cope with an entirely new environment by adaptively mixing pre-existing motor primitives as multiple internal models. However, the central nervous system (CNS) must solve a selection problem: deciding which internal models are appropriate for usage and learning under a given context of sensory-motor behaviors. MOSAIC models have been proposed for the learning and switching of internal models (Wolpert and Kawato, 1998; Kawato and Wolpert, 1998b; Wolpert et al., 1998, 2003; Wolpert and

Ghahramani, 2000; Haruno et al., 2001; Doya et al., 2002). In this model, output from multiple internal models are mixed in proportion to their appropriateness for the current context. Therefore, an enormous repertoire of behavior can be generated even if the number of internal models is limited, and many situations that we encounter may be derived from a combination of previously experienced situations. A recent study (Imamizu et al., 2004) suggests that the dorsolateral prefrontal (area 46) and the parietal regions contribute to the selection and combination ('blending') of multiple internal models. A PET study on monkeys also found that fronto-cerebellar interaction contributes to switching tools when monkeys use several tools simultaneously (Obayashi et al., 2002). A recent neuroanatomical study (Kelly and Strick, 2003) found loop connections between area 46 and the cerebellum, which is consistent with these results.

Based on a series of previous studies that we have conducted, the results of our current study can be interpreted as follows. Before scanning brain activity, an internal model for the 60° joystick and one for the 160° joystick were acquired in the cerebellum as a result of long-term training. In the pre-test, it was assumed that the CNS copes with the new 110° joystick by blending the output from the 60° and the 160° internal models. Activation in area 46 and the parietal regions contributed to this blending process. An increase in 110° activity was observed in the premotor regions, in the SMA, and in the inferior part of the cerebellum in the post-test in comparison to pre-tests, suggesting that an internal model for the 110° joystick was acquired in these regions. For the following reasons, it is assumed that internal models are acquired in the inferior part of the cerebellum. First, group analysis (random effect analysis) indicated that the volume increase was the largest in lobule 7b of the inferior cerebellum (from 15 to 686 + 11 voxels, Table I). Second, a marginally significant increase of activation was identified only in the inferior cerebellum among the regions where the quantitative analysis was conducted (Figure 7). As mentioned above, a previous study that we conducted indicated that functional connectivity between the lateral parts of the cerebellum and the premotor regions increased after acquisition of the internal model, which suggests that the acquired internal models send outputs to the premotor regions (Tamada et al., 1999). Electrophysiological studies (e.g., Sasaki et al., 1977) and neuroanatomical studies (Middleton and Strick, 1994; Kelly and Strick, 1998; Dum and Strick, 2003) have revealed reciprocal connections between the cerebellar and premotor regions. It is supposed that internal models for the 60° and 160° joysticks had already been acquired in the pre-test and that these models sent outputs to the premotor regions. The connectivity probably further increased in the post-test after acquisition of the 110° internal

1 model. Our study suggested that the SMA also
 2 receives outputs from the acquired internal models.
 3 The 60° and the 110° internal models contributed to
 4 manipulation of the 110° joystick in the pre-test,
 5 but it is unknown whether these models contributed
 6 to learning the 110° internal models.

7 The results of our current experiments do not
 8 contradict the following computational
 9 interpretations. When encountering a new tool, the
 10 CNS attempts to cope with it by blending outputs
 11 from internal models previously acquired. The
 12 prefrontal and parietal regions receive outputs from
 13 the internal models and contribute to the blending.
 14 However, after the acquisition of a proper internal
 15 model, the output of the internal model is directly
 16 sent to the premotor regions. Our findings suggest
 17 that the acquisition of a new cognitive function
 18 causes reorganization in the lateral cerebellum and
 19 changes global information flow in the cerebro-
 20 cerebellar communication loop.

21
 22 *Acknowledgements.* This research was supported in
 23 part by the National Institute of Information and
 24 Communications Technology.

25 REFERENCES

26
 27 BUONOMANO DV and MERZENICH MM. Cortical plasticity: From
 28 synapses to maps. *Annual Review of Neuroscience*, 21: 149-
 29 186, 1998.
 30 DESMOND JE and FIEZ JA. Neuroimaging studies of the
 31 cerebellum: Language, learning and memory. *Trends in*
 32 *Cognitive Science*, 2: 355-362, 1998.
 33 DESMOND JE, GABRIELI JD, WAGNER AD, GINIER BL and GLOVER
 34 GH. Lobular patterns of cerebellar activation in verbal
 35 working-memory and finger-tapping tasks as revealed by
 36 functional MRI. *Journal of Neuroscience*, 17: 9675-9685,
 37 1997.
 38 DOYA K, SAMEJIMA K, KATAGIRI K and KAWATO M. Multiple
 39 model-based reinforcement learning. *Neural Computation*, 14:
 40 1347-1369, 2002.
 41 DUM RP and STRICK PL. An unfolded map of the cerebellar
 42 dentate nucleus and its projections to the cerebral cortex.
 43 *Journal of Neurophysiology*, 89: 634-639, 2003.
 44 ELBERT T, PANTEV C, WIENBRUCH C, ROCKSTROH B and TAUB E.
 45 Increased cortical representation of the fingers of the left hand
 46 in string players. *Science*, 270: 305-307, 1995.
 47 GRAFMAN J, LITVAN I, MASSAQUOI S, STEWART M, SIRIGU A and
 48 HALLETT M. Cognitive planning deficit in patients with
 49 cerebellar atrophy. *Neurology*, 42: 1493-1496, 1992.
 50 HARUNO M, WOLPERT DM and KAWATO M. Multiple paired
 51 forward-inverse models for sensorimotor learning and control.
 52 *Neural Computation*, 13: 2201-2220, 2001.
 53 IMAMIZU H, KURODA T, MIYAUCHI S, YOSHIOKA T and KAWATO M.
 54 Modular organization of internal models of tools in the human
 55 cerebellum. *Proceedings of National Academy of Sciences of*
 56 *the USA*, 100: 5461-5466, 2003.
 57 IMAMIZU H, KURODA T, YOSHIOKA T and KAWATO M. Functional
 58 magnetic resonance imaging examination of two modular
 59 architectures for switching multiple internal models. *Journal*
 60 *of Neuroscience*, 24: 1173-1181, 2004.
 61 IMAMIZU H, MIYAUCHI S, TAMADA T, SASAKI Y, TAKINO R, PUTZ B,
 YOSHIOKA T and KAWATO M. Modular organization of
 multiple internal models for visuomotor learning: A functional
 MRI study. *Abstracts Society for Neuroscience*, 24: 166, 1998.
 IMAMIZU H, MIYAUCHI S, TAMADA T, SASAKI Y, TAKINO R, PUTZ B,
 YOSHIOKA T and KAWATO M. Human cerebellar activity
 reflecting an acquired internal model of a new tool. *Nature*,
 403: 192-195, 2000.
 JENKINS WM, MERZENICH MM, OCHS MT, ALLARD T and GUIC-
 ROBLES E. Functional reorganization of primary
 somatosensory cortex in adult owl monkeys after behaviorally
 controlled tactile stimulation. *Journal of Neurophysiology*, 63:
 82-104, 1990.
 KARNI A, MEYER G, JEZZARD P, ADAMS MM, TURNER R and

UNGERLEIDER LG. Functional MRI evidence for adult motor
 cortex plasticity during motor skill learning. *Nature*, 377: 155-
 158, 1995.
 KARNI A, MEYER G, REY-HIPOLITO C, JEZZARD P, ADAMS MM,
 TURNER R and UNGERLEIDER LG. The acquisition of skilled
 motor performance: Fast and slow experience-driven changes
 in primary motor cortex. *Proceedings of National Academy of*
Sciences of the USA, 95: 861-868, 1998.
 KAWATO M and WOLPERT DM. Internal models for motor control.
Novartis Foundation Symposium, 218: 291-304 (discussion
 304-307), 1998a.
 KAWATO M and WOLPERT DM. Internal models for motor control.
 In Glickstein M (Ed), *Sensory Guidance of Movement*.
 Sussex: John Wiley & Sons, 1998b.
 KELLY RM and STRICK PL. Cerebro-cerebellar "loops" are closed.
Abstracts Society for Neuroscience, 24: 1407, 1998.
 KELLY RM and STRICK PL. Cerebellar loops with motor cortex and
 prefrontal cortex of a nonhuman primate. *Journal of*
Neuroscience, 23: 8432-8444, 2003.
 KIM SG, UGURBIL K and STRICK PL. Activation of a cerebellar
 output nucleus during cognitive processing. *Science*, 265:
 949-951, 1994.
 MIDDLETON FA and STRICK PL. Anatomical evidence for cerebellar
 and basal ganglia involvement in higher cognitive function.
Science, 266: 458-461, 1994.
 OBAYASHI S, SUHARA T, KAWABE K, OKAUCHI T, MAEDA J, AKINE
 Y, ONOE H and IRIKI A. Functional brain mapping of monkey
 tool use. *NeuroImage*, 14: 853-861, 2001.
 OBAYASHI S, SUHARA T, NAGAI Y, MAEDA J, HIHARA S and IRIKI A.
 Macaque prefrontal activity associated with extensive tool
 use. *Neuroreport*, 13: 2349-2354, 2002.
 OLDFIELD RC. The assessment and analysis of handedness: The
 Edinburgh inventory. *Neuropsychologia*, 9: 97-113, 1971.
 PETERSEN SE, FOX PT, POSNER MI, MINTUM M and RAICHLER ME.
 Positron emission tomographic studies of the processing of
 single words. *Journal of Cognitive Neuroscience*, 1: 153-170,
 1989.
 RAICHLER ME, FIEZ JA, VIDEEN TO, MACLEOD AM, PARDO JV, FOX
 PT and PETERSEN SE. Practice-related changes in human brain
 functional anatomy during nonmotor learning. *Cerebral*
Cortex, 4: 8-26, 1994.
 SAKAI K, TAKINO R, HIKOSAKA O, MIYAUCHI S, SASAKI Y, PUTZ B
 and FUJIMAKI N. Separate cerebellar areas for motor control.
Neuroreport, 9: 2359-2363, 1998.
 SASAKI K, OKA H, KAWAGUCHI S, JINNAI K and YASUDA T. Mossy
 fibre and climbing fibre responses produced in the cerebellar
 cortex by stimulation of the cerebral cortex in monkeys.
Experimental Brain Research, 29: 419-428, 1977.
 SHUMWAY CA, MORISSETTE J, GRUEN P and BOWER JM. Plasticity
 in cerebellar tactile maps in the adult rat. *Journal of*
Comparative Neurology, 413: 583-592, 1999.
 TAMADA T, MIYAUCHI S, IMAMIZU H, YOSHIOKA T and KAWATO M.
 Cerebro-cerebellar functional connectivity revealed by the
 laterality index in tool-use learning. *Neuroreport*, 10: 325-
 331, 1999.
 THACH WT. On the specific role of the cerebellum in motor
 learning and cognition: Clues from PET activation and lesion
 studies in man. *Behavioral and Brain Sciences*, 19: 411-431,
 1996.
 TZOURIO-MAZOYER N, LANDEAU B, PAPATHANASSIOU D, CRIVELLO
 F, ETARD O, DELCROIX N, MAZOYER B and JOLIOU M.
 Automated anatomical labeling of activations in SPM using a
 macroscopic anatomical parcellation of the MNI MRI single-
 subject brain. *NeuroImage*, 15: 273-289, 2002.
 VAN MIER H, TEMPEL LW, PERLMUTTER JS, RAICHLER ME and
 PETERSEN SE. Changes in brain activity during motor learning
 measured with PET: Effects of hand of performance and
 practice. *Journal of Neurophysiology*, 80: 2177-2199, 1998.
 WOLPERT DM, DOYA K and KAWATO M. A unifying computational
 framework for motor control and social interaction.
Philosophical Transactions of the Royal Society of London B,
 358: 593-602, 2003.
 WOLPERT DM and GHAHRAMANI Z. Computational principles of
 movement neuroscience. *Nature Neuroscience*, 3: S1212-
 S1217, 2000.
 WOLPERT DM and KAWATO M. Multiple paired forward and
 inverse models for motor control. *Neural Networks*, 11: 1317-
 1329, 1998.
 WOLPERT DM, MIALL RC and KAWATO M. Internal models in the
 cerebellum. *Trends in Cognitive Sciences*, 2: 338-347, 1998.